

**HYDROACOUSTIC BLOCKAGE AT DIEGO GARCIA:
MODELS AND OBSERVATIONS**

Jay J. Pulli and Zachary M. Upton

BBN Technologies

Sponsored by National Nuclear Security Administration
Office of Nonproliferation Research and Engineering
Office of Defense Nuclear Nonproliferation

Contract No. DE-AC04-2000AL66933

ABSTRACT

Hydroacoustic blockage occurs when a bathymetric feature (island, atoll or seamount) is in the path of propagating acoustic energy. An understanding of hydroacoustic blockage is essential when planning an array location, mapping detection and localization coverage, and interpreting hydroacoustic reflection data. The new hydroacoustic array at Diego Garcia, which actually consists of two sub-arrays on either side of the atoll, provides an excellent opportunity for evaluating model predictions of blockage using the recordings of T-waves from shallow earthquakes in the Indian Ocean.

The latest release of HydroCAM, our long-range hydroacoustic modeling program, includes the Sandwell and Smith 2-minute-resolution bathymetry database. To model hydroacoustic blockage at Diego Garcia, we used this capability to perform a series of fan-ray calculations for both sub-arrays at 2-degree azimuth increments. These rays were compared with previous calculations using the ETOPO5 5-minute grid, both to verify the database integration and to compare the two databases. We used two criteria for hydroacoustic blockage:

- The bathymetry is shallower than 50 meters (thereby blocking most propagating acoustic energy).
- The bathymetry is shallower than the Sound Channel Axis depth in the region (thereby blocking acoustic energy in the SCA).

These criteria result in binary blockage evaluations; that is, either the ray path is blocked or it is not. However, observations indicate that the process of blockage is more complicated. For example, ray paths coming from the north should be blocked by the atoll and not be observed at the south array. Acoustic data from the south array shows that although the energy is attenuated, arrivals can easily be identified.

In order to resolve some of the modeling issues, we have compiled a waveform database of about three dozen shallow earthquakes in the Indian Ocean recorded by the Diego Garcia subarrays. These events cover nearly all azimuths around Diego Garcia. Using this dataset, we have computed a 360-degree blockage chart for Diego Garcia that shows the frequency dependence of energy attenuation around the atoll. We have also suggested some improvements to the models that will improve our blockage prediction capability.

KEY WORDS: hydroacoustics, Diego Garcia, Indian Ocean, blockage

OBJECTIVE

The objective of this research is to model hydroacoustic blockage around Diego Garcia. An understanding of hydroacoustic blockage is essential when planning an array location, mapping detection and localization coverage, and interpreting hydroacoustic reflection data. Model predictions were made using the latest version of our program HydroCAM with two different path blockage criteria. These predictions were then compared with actual observations using a dataset of earthquake sources around the Indian Ocean. A methodology was developed to correct each observation for earthquake magnitude and distance from Diego Garcia.

RESEARCH ACCOMPLISHED

Model Predictions of Blockage Using HydroCAM

Hydroacoustic blockage was modeled at both Diego Garcia subarrays using the latest version (3.3) of the program HydroCAM. We performed a series of fan-ray calculations for both sub-arrays at 2-degree azimuth increments using two bathymetric databases. The first database was the ETOPO5 5-minute resolution grid; the second was the Sandwell and Smith 2-minute resolution grid. Two criteria were used to determine blockage: one was when the bathymetry is shallower than 50 meters (thereby blocking most propagating acoustic energy); the second was when the bathymetry is shallower than the Sound Channel Axis depth in the region (thereby blocking acoustic energy in the SCA). Results of these eight combinations are shown in Figures 1 and 2.

Although the gross features of the predictions are similar, there are important differences. For both of the sub arrays, the widest azimuthal coverage is predicted by the ETOP5 bathymetry database and the 50-meter stop criterion. The smallest azimuthal coverage is predicted by the ETOP5 bathymetry database and the SCA stop criterion. These varying results point to either the need for higher resolution bathymetry around Diego Garcia, better stop criteria, or both. Our goal here to compare these predictions with actual observations.

Observations: Events Analyzed

As of this writing, hydroacoustic data from 27 events in the Indian Ocean area have been analyzed. A list of these events is given in Table 1 and a corresponding epicentral map is shown in Figure 3. The event distribution in distance and azimuth is shown in Figure 4. Clearly, we have gaps in the azimuthal coverage for the northeast, southeast, and west directions from the array. We hope to fill these gaps as time goes on and more events are recorded. For each event, 2-3 hours of waveform data (starting at the origin time) were obtained for all six hydrophones at Diego Garcia. The waveform data are sampled at 250 Hz. The analysis process consists of three steps. First, the waveform data are converted to waveform envelopes, from which the amplitudes of the T-waves are measured. Next, these amplitudes must be scaled to account for the fact that the events are of varying magnitude. Finally, the amplitudes must be corrected for propagation losses, given that the events are of varying distances from Diego Garcia. Once these steps are accomplished, an assessment of blockage around Diego Garcia can be undertaken.

Data Processing

Data processing for this analysis consisted of the conversion from full band calibrated waveform data to waveform envelopes. This was accomplished by first detrending the data, then filtering in the passband of 3 to 30 Hz. (Noise dominates the signal below 3 Hz and there is little energy above 30 Hz.) The filtered data were then rectified (absolute value) and smoothed over a 2-second window that was stepped down the time series one sample at a time. This smoothed envelope was then subsampled to a rate of one sample per second. The waveform envelopes for each of the three sensors at each sub array were then averaged. T-wave amplitudes were measured at the peak of the envelope, which corresponds to the arrival time of Mode 1 (sound channel axis propagation). An example is shown in Figure 5. In order to measure blockage, we must first scale the measured T-wave amplitudes to account for differences in event magnitudes and distances from the arrays.

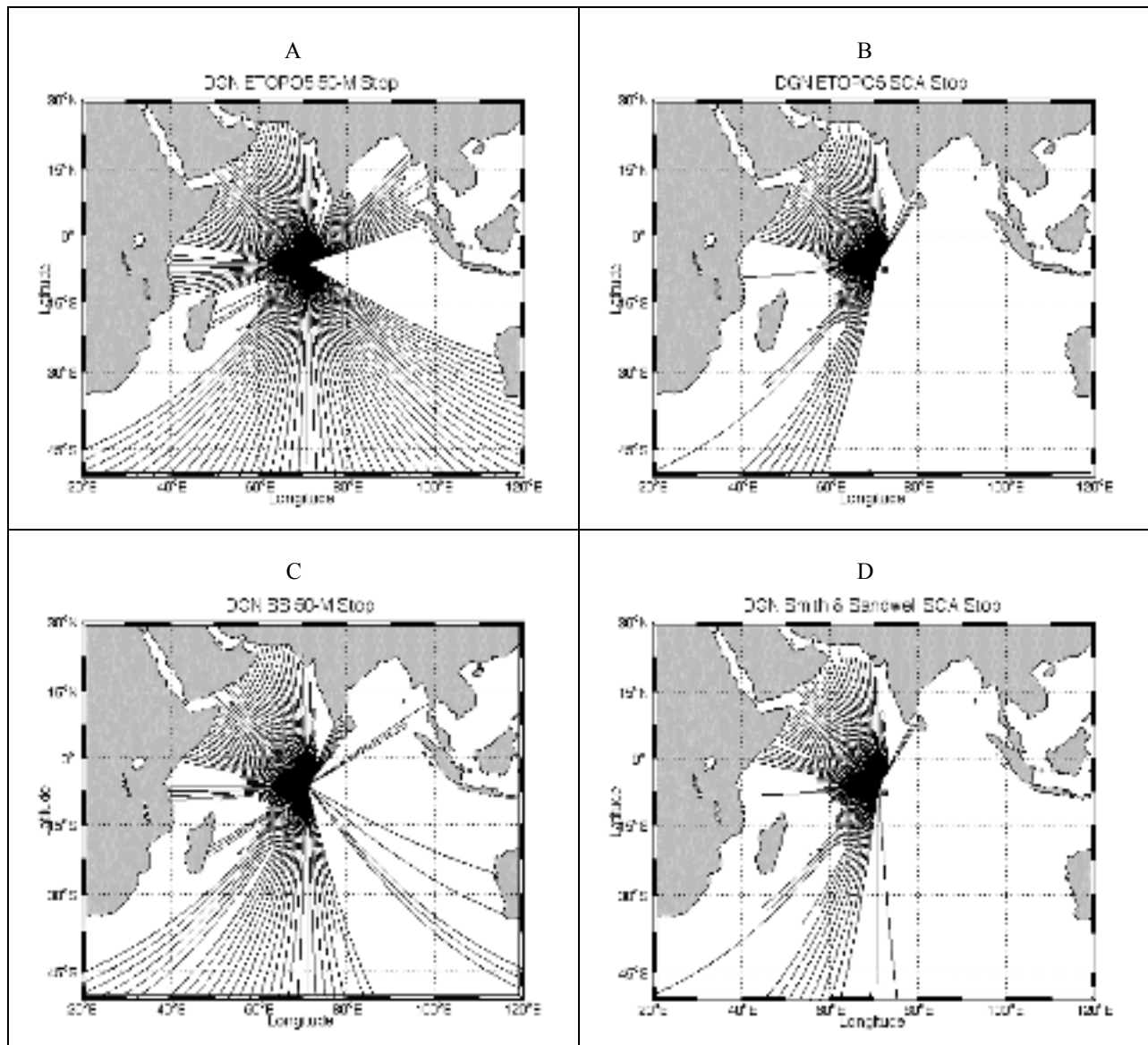


Figure 1. Four fan-ray calculations at Diego Garcia North using HydroCAM: A) ETOPO5 bathymetry database with a ray stop criterion of 50-m depth. B) ETOPO5 database with a ray stop criterion of the Sound Channel Axis (SCA) depth equaling that of the bathymetry. C) Smith and Sandwell bathymetry database with a ray stop criterion of 50-m depth. D) Smith and Sandwell database with a ray stop criterion of the SCA depth equaling that of the bathymetry.

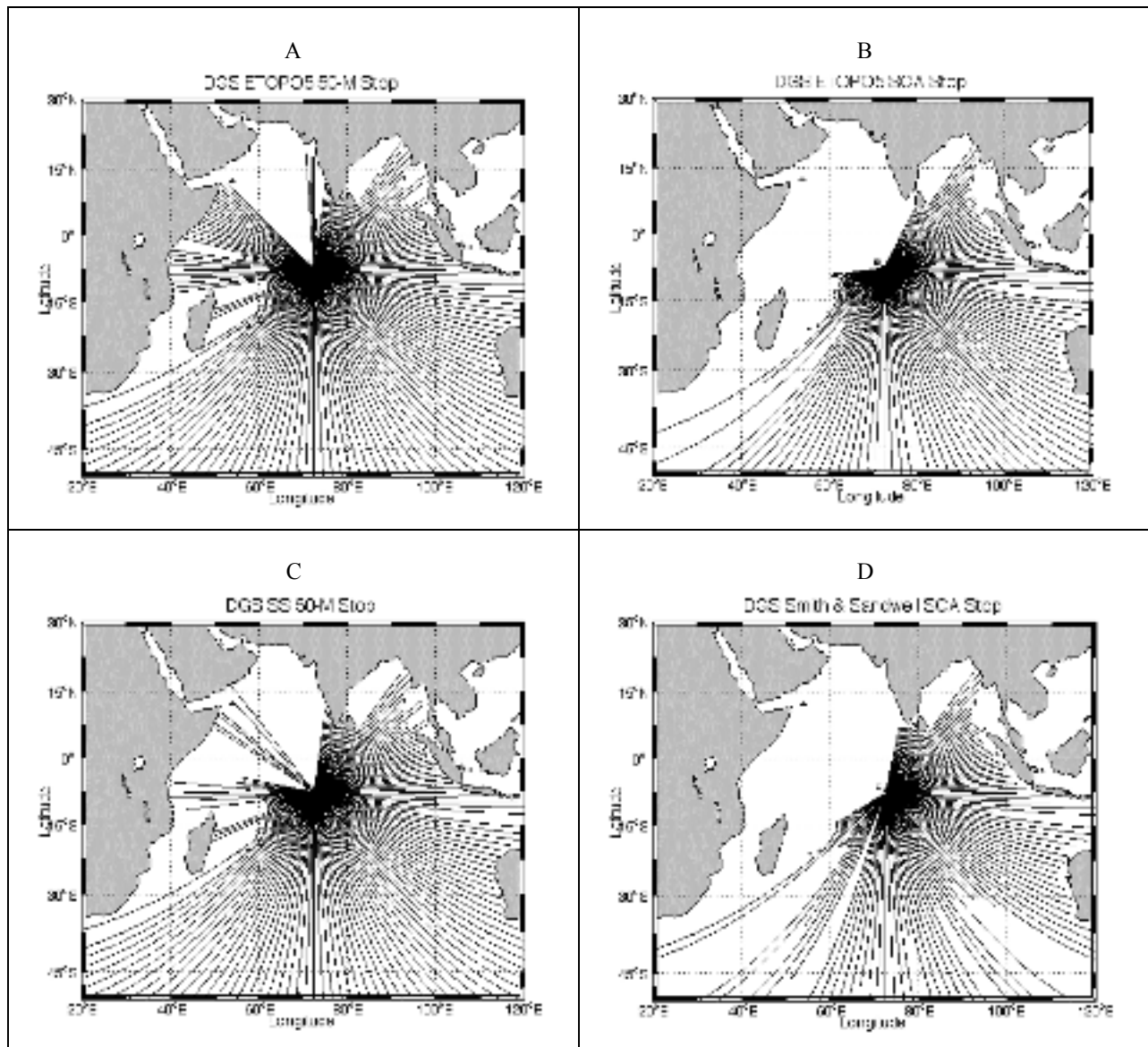


Figure 2. Four fan-ray calculations at Diego Garcia South using HydroCAM: A) ETOPO5 bathymetry database with a ray stop criterion of 50-m depth. B) ETOPO5 database with a ray stop criterion of SCA depth equaling that of the bathymetry. C) Smith and Sandwell bathymetry database with a ray stop criterion of 50-m depth. D) Smith and Sandwell database with a ray stop criterion of the SCA depth equaling that of the bathymetry.

<u>Yr/Mo/Dy</u>	<u>Hr:Mn:Sc</u>	<u>Lat.</u>	<u>Long.</u>	<u>Depth km</u>	<u>Mag m_b</u>	<u>Geographic Area</u>
2001/01/26	03:16:40	23.42	70.23	16.0	7.8	Gujarat, India
2001/01/26	07:32:28	23.42	69.98	10.0	5.5	Gujarat, India
2001/01/28	01:02:10	23.51	70.52	10.0	5.9	Gujarat, India
2001/02/14	19:28:03	-4.68	102.56	36.0	7.2	Sumatera
2001/02/15	10:04:36	23.27	70.29	10.0	4.7	Gujarat, India
2001/03/11	07:06:03	-4.28	89.06	10.0	4.9	South Indian Ocean
2001/03/13	13:48:19	23.73	69.56	10.0	3.7	Gujarat, India
2001/03/25	07:14:08	14.09	53.46	10.0	4.9	Owen Fracture Zone
2001/03/30	07:24:19	-41.98	88.44	10.0	5.1	Southeast Indian Rise
2001/03/31	02:26:30	3.99	95.94	33.0	5.2	W Coast of N Sumatera
2001/04/04	07:26:32	-34.26	55.46	10.0	5.0	Southwest Indian Ridge
2001/04/04	13:06:13	-34.38	55.43	10.0	5.6	Southwest Indian Ridge
2001/04/08	19:26:43	-11.76	65.98	10.0	5.0	Mid-Indian Ridge
2001/04/08	10:54:09	-25.12	67.65	10.0	5.1	Indian Ocean Triple Junction
2001/04/16	14:25:59	23.44	70.12	10.0	4.1	Gujarat, India
2001/04/19	00:44:10	-14.63	66.21	10.0	4.9	Mid-Indian Ridge
2001/04/23	16:35:35	13.21	50.50	10.0	5.2	Eastern Gulf of Aden
2001/04/25	21:02:43	-8.92	106.47	33.0	5.5	South of Jawa, Indonesia
2001/05/04	01:10:48	-33.59	57.19	10.0	5.0	SW Indian Ridge
2001/05/11	22:18:02	0.67	98.58	33.0	5.4	Northern Sumatera
2001/05/18	02:05:34	0.47	97.80	33.0	5.9	Northern Sumatera
2001/05/25	05:05:59	-7.91	110.26	33.0	5.9	Jawa, Indonesia
2001/05/31	20:23:42	9.80	57.68	10.0	4.6	Carlsberg Ridge
2001/06/15	16:19:07	13.76	51.69	10.0	5.7	Eastern Gulf of Aden
2001/06/21	14:19:19	22.93	69.65	10.0	4.5	Gujarat, India
2001/06/28	03:46:27	-6.91	108.30	33.0	5.0	Jawa, Indonesia

Table 1. List of events used for the blockage analysis. An epicentral map is shown in Figure 3. Epicentral data sources include the NEIS and IRIS databases.

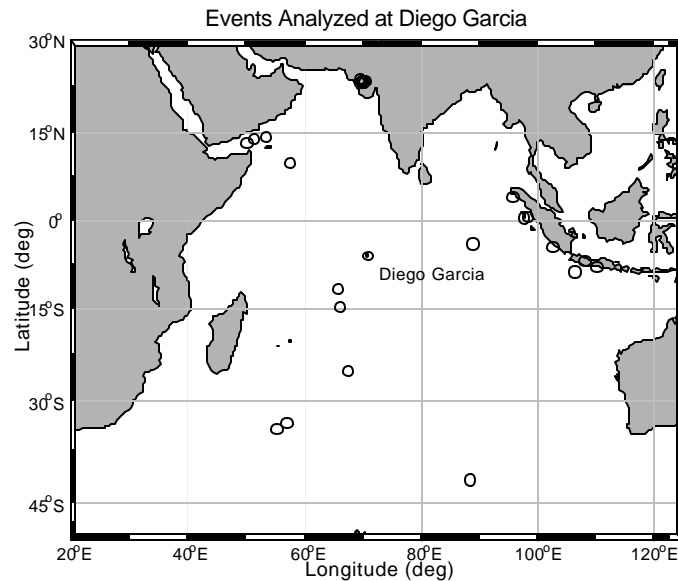


Figure 3. Epicenters of the events measured in this study. See Table 1.

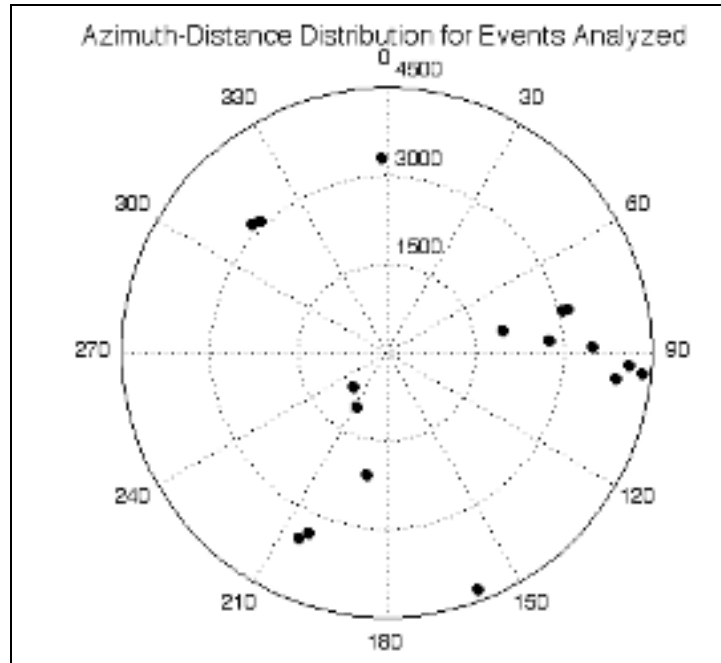


Figure 4. Azimuth-distance distribution for the events studied at Diego Garcia. As of this writing, there are gaps in the azimuthal coverage to the northeast, southeast, and west of the array.

T-Wave Amplitude vs. Seismic Magnitude

The next step in the analysis is the conversion of the measured T-wave amplitudes to their equivalent amplitudes for an event of a given magnitude. To accomplish this, we used the measured T-wave amplitudes for the January 26, 2001, western India earthquake and its aftershocks. Since all of these events are roughly the same distance from Diego Garcia (3280 km), transmission losses will be the same for each event; hence, amplitude differences will solely be the function of earthquake magnitude. (This, of course, ignores any amplitude variation due to differences in source mechanism or source depth.) T-wave amplitudes at the Diego Garcia north array for ten events in the western India source zone are plotted in Figure 6. Seismic magnitudes were taken from NEIS epicenter lists. As expected, there is a linear relationship between T-wave amplitude in dB and seismic magnitude. This relationship, for the fixed epicentral distance of 3280 km to Diego Garcia, is

$$\text{dB} = 54.7 + 12.4 m_b$$

Note from Figure 4 that with a measured background noise level of 95 dB at Diego Garcia, we would expect to observe T-waves from events in the source region as small as magnitude 3.2. Based on this result, we can now derive a correction factor that will scale the measured T-wave amplitudes to those of an earthquake of a given seismic magnitude. Here we chose magnitude 5 as our standard event magnitude. This relationship is

$$\text{dB}(m_b=5) = \text{dB} - 12.4 + 54.7 m_b$$

T-Wave Amplitude vs. Distance

Once the T-wave amplitudes have been scaled to a common event magnitude, they must next be corrected for propagation losses to a common distance. This can be accomplished using the equation (Urlick, 1983)

$$TL = 60 + 10\log_{10}r + 0.00333r$$

for Mode-1 transmission loss (TL) in the sound channel axis. Here, TL is in dB, and r is the distance in kilometers. This equation accounts for both geometrical spreading and attenuation. (Attenuation losses are very small in the sound channel axis, amounting to only 3.3 dB per 1000 km of propagation.)

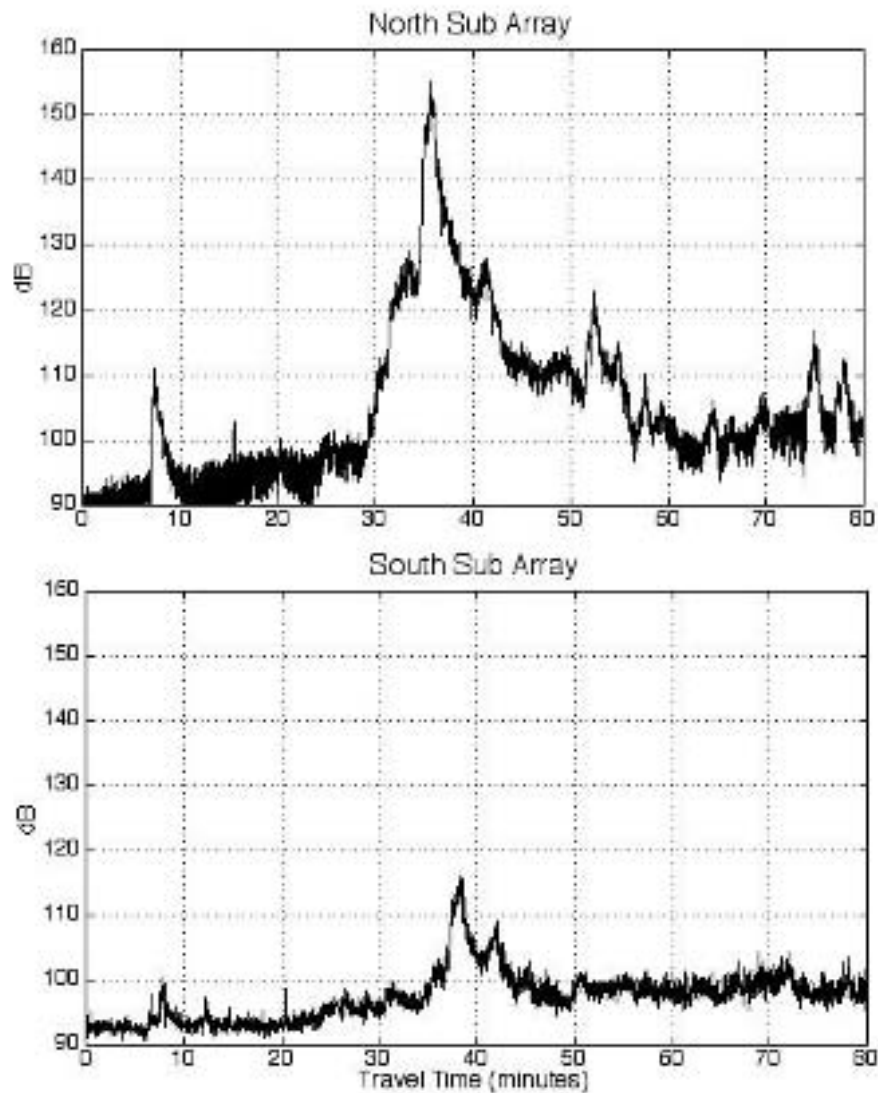


Figure 5. T-wave envelopes computed from Diego Garcia data for January 26, 2001, Guinart, India. The T-wave travel time is approximately 37 minutes to Diego Garcia North (top). The arrival at 8 minutes is the conversion from seismic P-wave below the array to acoustic energy (see Pulli and Upton, 2001). Three of the four predictions for Diego Garcia South indicate that T-waves will be blocked from this azimuth; however T-wave energy is recorded at the South array, albeit at a level that is approximately 40 dB below that at the North array.

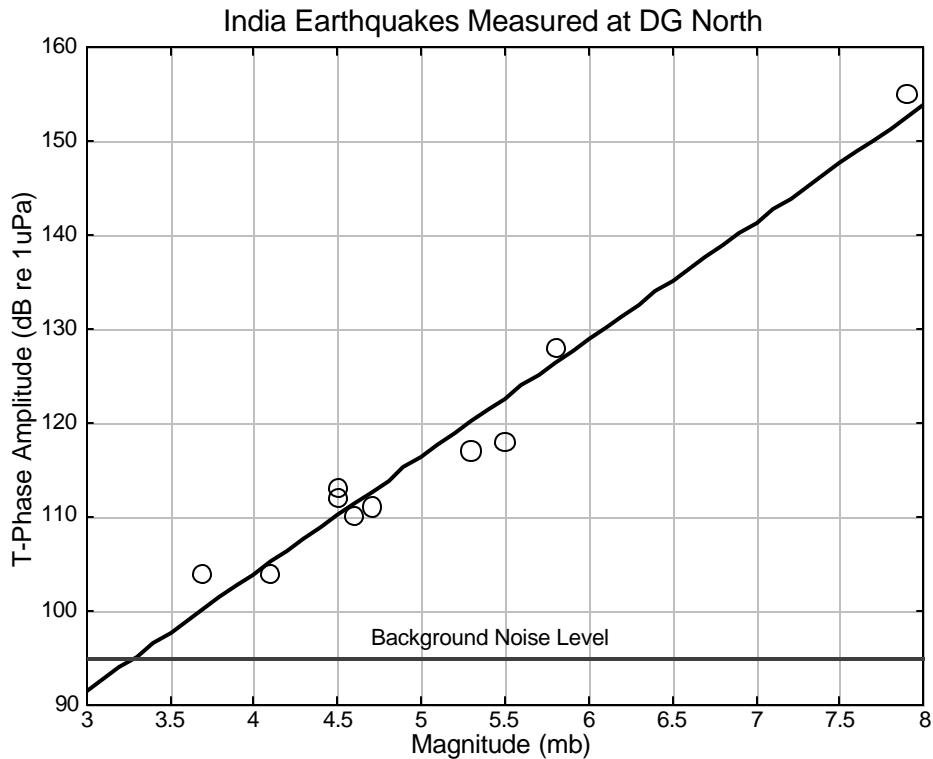


Figure 6. Amplitudes of T-waves in dB measured at the Diego Garcia north array for the January 26, 2001, western India earthquakes and some of its aftershocks. All events are 3280 km from the array.

T-Wave Amplitudes Around Diego Garcia

The measured T-wave amplitudes, corrected to a common magnitude 5 event and scaled for transmission loss, are plotted as a function of azimuth in Figure 7 (for the north array) and Figure 8 (for the south array). Note that transmission losses were not applied to signals that were completely blocked, which would only serve to artificially increase amplitudes at a given subarray. For the north subarray, the most important observation is that we see T-waves coming from the east, whereas all of the predictions from Figure 1 indicate that paths to the east should be blocked. For the south subarray, we see T-waves coming from the northwest, whereas all of the predictions from Figure 2 indicate that paths to the east should be blocked.

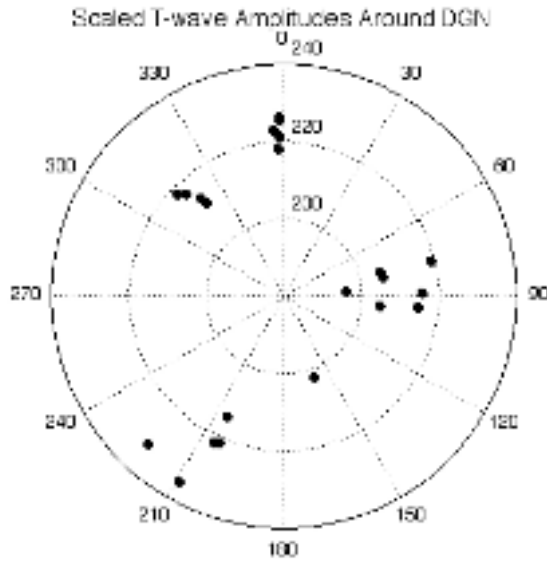


Figure 7. Observed T-wave amplitudes at Diego Garcia North subarray. The amplitudes have been scaled to a common event magnitude (5.0) and corrected for transmission losses.

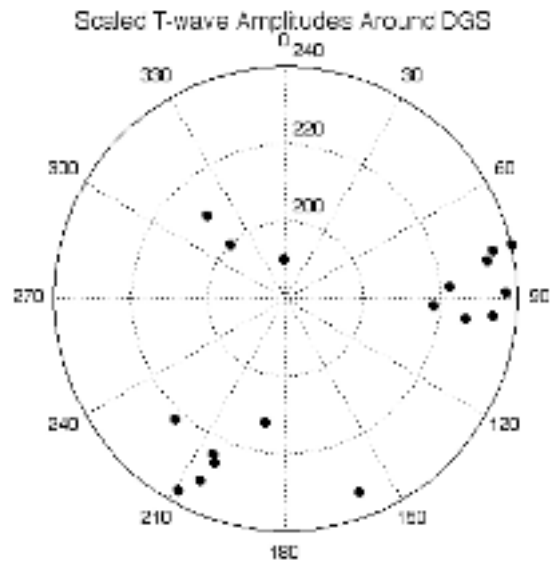


Figure 8. Observed T-wave amplitudes at Diego Garcia South sub array. The amplitudes have been scaled to a common event magnitude (5.0) and corrected for transmission losses.

CONCLUSIONS AND RECOMMENDATIONS

Our studies of the prediction of hydroacoustic blockage at Diego Garcia, and our observations based on T-waves from earthquakes in the Indian Ocean area, lead us to draw the following conclusions:

1. The predictions of hydroacoustic blockage around Diego Garcia vary, depending on the resolution of the bathymetry used and the criterion for blockage.
2. In some cases, we observe T-waves at a Diego Garcia sub array where the predictions indicate that none should be observed.
3. A better definition of "hydroacoustic blockage" is required which goes beyond the binary blocked/unblocked

We recommend:

1. Continued accumulation of waveform data at Diego Garcia in order to fill in the coverage gaps that exist in our analysis. Recordings of events in the northeast, southeast, and west directions from Diego Garcia are required.
2. As higher resolution bathymetric databases become available for this region, they should be integrated into HydroCAM.
3. Modeling of the diffraction and scattering of hydroacoustic energy around Diego Garcia should be undertaken.
4. Further acoustical analysis, in the form of modal or PE modeling, should be conducted to discover and evaluate better blockage criteria.

REFERENCES

GDEM (1995), Database Description for the Master Generalized Digital Environment Model (GDEM) Version 5.0, OAML DBD-20F, Naval Oceanographic Office, Stennis Space Center MS. September 1995.

Pulli, J.J. and Z. Upton (2001), Hydroacoustic observations of the January 26, 2001 Western India earthquake and its aftershocks, presented at the Spring Meeting of the American Geophysical Union, Boston, MA.

Smith, W. H. F. and D. T. Sandwell (1997), Global Sea Floor Topography from Satellite Altimetry and Ship Depth Soundings, *Science*, **277**, p. 1956-1962.

Urick, R.J. (1983), Principles of Underwater Sound, 3rd ed., McGraw-Hill Book Company, NY.